Tellus (2001), 53B, 103–121
Printed in UK. All rights reserved

Copyright © Munksgaard, 2001
TELLUS
ISSN 0280–6509

Future changes of the atmospheric composition and the impact of climate change

By VOLKER GREWE[1,2]*, MARTIN DAMERIS[1], RALF HEIN[1], ROBERT SAUSEN[1] and BENEDIKT STEIL[3,4], [1]*DLR Institut für Physik der Atmosphäre, Oberpfaffenhofen, D-82234 Weßling, Germany;* [2]*NASA-Goddard Institute of Space Studies/Columbia University, New York, New York 10025, USA;* [3]*Max-Planck-Institute for Chemistry, PF 3060, D-55020 Mainz, Germany;* [4]*Now at Max-Planck-Institute for Meteorology, Bundesstr. 55, D-20146 Hamburg, Germany*

(Manuscript received 29 February 2000; in final form 11 November 2000)

ABSTRACT

The development of the future atmospheric chemical composition is investigated with respect to NO_y and O_3 by means of the off-line coupled dynamic-chemical general circulation model ECHAM3/CHEM. Two time slice experiments have been performed for the years 1992 and 2015, which include changes in sea surface temperatures, greenhouse gas concentrations, emissions of CFCs, NO_x and other species, i.e., the 2015 simulation accounts for changes in chemically relevant emissions and for a climate change and its impact on air chemistry. The 2015 simulation clearly shows a global increase in ozone except for large areas of the lower stratosphere, where no significant changes or even decreases in the ozone concentration are found. For a better understanding of the importance of (A) emissions like NO_x and CFCs, (B) future changes of air temperature and water vapour concentration, and (C) other dynamical parameters, like precipitation and changes in the circulation, diabatic circulation, stratosphere–troposphere-exchange, the simulation of the future atmosphere has been performed stepwise. This method requires a climate-chemistry model without interactive coupling of chemical species. Model results show that the direct effect of emissions (A) plays a major rôle for the composition of the future atmosphere, but they also clearly show that climate change (B and C) has a significant impact and strongly reduces the NO_y and ozone concentration in the lower stratosphere.

1. Introduction

The concentrations of atmospheric trace gases like CO_2, N_2O, CH_4, NO_x ($= NO + NO_2$), and O_3 are linked to climate in several ways. On the one hand side, greenhouse gases lead to a change in atmospheric radiation fluxes and furthermore in climate (IPCC, 1996). On the other hand a change in climate, i.e., temperature, circulation, hydrological cycle, etc., has an impact on the distribution of chemical species (changes in transport) and chemical reaction rates, and therefore it has an impact on the chemical composition of the atmosphere. Most studies, which deal with climate-chemistry interactions focus on the first aspect, especially on the effect of the main anthropogenically increased greenhouse gases CO_2, N_2O, and CH_4 (IPCC, 1996), but also on ozone (Fishman et al., 1979; a summary can be found in Ramanathan et al., 1987 and Roelofs et al., 1999).

Studies concentrating on the effect of a climate change on atmospheric trace gas concentrations mostly regard stratospheric processes, e.g., the effect of CO_2 doubling on ozone (Brasseur et al., 1990; Shindell et al., 1998a), and a delayed recovery

* Corresponding author.
e-mail: volker.grewe@dlr.de

of the ozone layer due to a decrease in stratospheric temperatures and a change in wintertime circulation (Shindell et al., 1998b; Dameris et al., 1998a).

Tropospheric climate-chemistry interactions on the basis of a 2-D climate-chemistry model were investigated by focusing on carbon monoxide (Wang and Prinn, 1999) as well as other species, e.g., NO_x (Wang and Prinn, 1997). They found indications that climate variations, especially those causing changes in the water vapour concentrations, can influence the future CO trends. Additionally they showed that climate change subtly impacts the future development of various trace gases, e.g., NO_x, due to a climate change induced increase of tropospheric OH and concluded that increasing emissions are causing primarily future changes in the atmospheric chemical composition.

The 3-D climate-chemistry model ECHAM3/CHEM was applied by Grewe et al. (1999a) to investigate the effect of a climate change on the atmospheric composition. They showed that in the period 1992 to 2015 tropospheric NO_x increases by 45% to 55%, resulting from a NO_x increase of 55% to 60% due to enhanced NO_x emissions and a decrease by 10% due to climate change. A decrease in ozone due to climate change was also found. Johnson et al. (1999) found qualitatively similar results by using the 3-D general circulation model HADAM2b, which was coupled with the Lagrangian chemistry transport model STOCHEM.

The present paper is based on Grewe et al. (1999a) and investigates the change in the concentrations of tropospheric O_3 and NO_y (= all atmospheric nitrogen compounds except for N_2 and N_2O), from 1992 to 2015, in more detail. It identifies processes responsible for future changes of the atmospheric composition. Fig. 1 shows a scheme of the investigated climate-chemistry interactions. Emissions of NO_x largely control the future change in NO_y and O_3 (process A). An increase of tropospheric temperature has a direct impact on chemical reaction rates and an increase of water vapour mixing ratios will change the abundance of OH radicals and therefore NO_y and O_3 concentrations (process B). Additionally, a change in cloud cover, liquid water content, precipitation, and circulation can lead to a change of the HNO_3 wash-out and rain-out, as well as

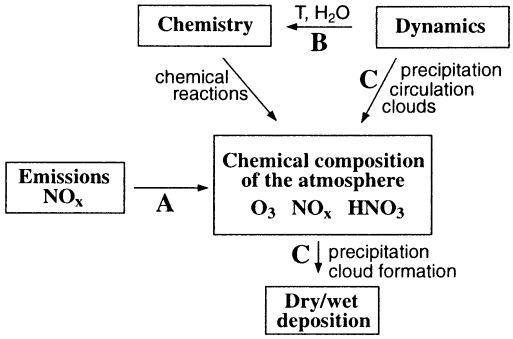

Fig. 1. Schematic view of the basic processes (A, B, and C) controlling the chemical composition of the atmosphere (see text for details).

stratosphere–troposphere ozone exchange (process C). Process A can be called a direct emission effect, since the emissions directly affect the chemistry, whereas processes B and C are indirect emission effects, since the emissions of greenhouse gases first change radiation and climate, which then modify atmospheric chemistry.

Since the thesis of a photo-chemical ozone source has been formulated (Fishman and Crutzen, 1978), tropospheric ozone attracted attention with regard to its climate impact (Fishman et al., 1979), and to past and possible future ozone changes (Hough and Derwent, 1990; Crutzen and Zimmermann, 1991). Recently, in a Special Report of the IPCC (1999) five 3-D chemical transport models (CTM) and one 3-D climate-chemistry model (ECHAM3/CHEM) were inter-compared (see also Stevenson et al., 1998 and Brasseur et al., 1998). For the period 1992 to 2015, an increase of the surface NO_x emissions of 45% for energy related sources and 7% for biomass burning was assumed. The CTM simulations showed an increase of the atmospheric ozone burden of 1.8 to 2.1 TgO_3 per emitted TgN in 2015 compared to 1992, which quantifies process A. The ECHAM3/CHEM model results of 1.8 TgO_3/TgN have been at the lower end of the CTM results.

Process B has been investigated by Toumi et al. (1996), who showed by means of a 2-D model that an increase in surface temperature lead to an enhancement of water vapour, which generally leads to a decrease in ozone, except in the northern lower troposphere. These findings were confirmed by 3-D studies by Grewe et al. (1999a) and

Johnson et al. (1999). Toumi et al. (1996) further showed that a change in lightning, which could be related to climate change, has an impact on ozone chemistry. As stated above, Wang and Prinn (1997, 1999) indicated that process C can have an impact on atmospheric chemistry. However, to provide more reliable answers to the questions of the potential impact of climate change on the atmospheric composition and predictions of the future atmosphere 3-D dynamic-chemical general circulation models for the troposphere and stratosphere have to be applied. Such models were not available until quite recently (Wuebbles, 1996). Here we apply the 3-D climate-chemistry model ECHAM3/CHEM. Future changes of upper troposphere NO_y and ozone are investigated, by analyzing the role of processes A, B, and C in detail. Since the interaction of dynamics, climate change and chemistry is highly non-linear, a full analysis of each process is beyond the scope of this paper. Instead, we focus on how each of the three processes influence the composition of the atmosphere and suggest underlying mechanisms. As a first step the coupling of the chemical and dynamic processes in the model is performed in an off-line mode, i.e., without feedback of the chemistry to radiation.

Section 2 gives a brief overview of the model ECHAM3/CHEM, including a validation of the derived NO_x, NO_y and O_3 concentrations, and describes the experimental set-up. Section 3 deals with the simulated climate change. The interactions of climate and chemistry are presented in Section 4, separated into the processes A, B, and C. Concluding remarks are given in Section 5.

2. Model and experimental set-up

2.1. Model description

The climate-chemistry model ECHAM3/CHEM (for details see Steil et al. (1998)) has already been used in studies focusing on the interaction between dynamics and chemistry (Grewe and Dameris, 1997; Grewe et al., 1998) and between climate change and chemistry (Dameris et al., 1998a and 1998b; Grewe et al., 1999a). Here we repeat only the main characteristics of ECHAM3 and CHEM.

2.1.1. Climate model ECHAM3. The atmosphere general circulation model ECHAM3 (Roeckner et al., 1992) generates its own climate, which only depends on the prescribed concentration of greenhouse gases (GHG) and sea surface temperatures (SST) (see Subsection 2.3 for details). Chemical species are transported using a semi-Lagrangian and mass-conserving advection scheme (Rasch and Williamson, 1990). A parameterization of the convective transport of chemical species is included (Tiedtke, 1989).

Since the present paper aims to investigate the impact of climate change on the chemical composition of the atmosphere, the employed model version does not include the feedback of chemical species on the dynamics. The calculated chemical species do not affect the radiative forcing of the dynamic fields (off-line mode). Rather, climate change is prescribed by GHGs and SSTs and its impact on the chemistry is investigated.

2.1.2. Chemistry module CHEM. The chemistry module CHEM (Steil, 1999) is based on the family concept. It includes 13 families and species that are transported: H_2O, CH_4, N_2O, HCl, H_2O_2, CO, CH_3O_2H, $ClONO_2$, HNO_3 + type I PSC ($= HNO_3 \cdot 3H_2O$), type II PSC (= water ice), ClO_x ($= Cl + ClO + HOCl + 2 \cdot Cl_2O_2 + 2 \cdot Cl_2$), NOX ($= N + NO + NO_2 + NO_3 + 2 \cdot N_2O_5 + HNO_4$), and O_x ($= O_3 + O(^3P) + O(^1D)$). Additionally, 17 species are treated (quasi-)diagnostically. The module CHEM considers a total of 107 photochemical reactions plus four heterogeneous reactions on parameterized polar stratospheric clouds (Hanson and Mauersberger, 1988) and two heterogeneous reactions on sulfate aerosol.

The wet deposition of HNO_3, HCl, and H_2O_2 is taken from Roelofs and Lelieveld (1995). In-cloud precipitation formation, evaporation, and below-cloud scavenging are considered for stratiform and convective clouds, provided by ECHAM3 at every timestep. Dry deposition velocities are taken from Dentener and Crutzen (1993) and Roelofs and Lelieveld (1995). CO, CH_4, and N_2O are prescribed at the surface. In the stratosphere NO_y and Cl_y zonal means are prescribed in the uppermost model level (centered at 10 hPa) including a seasonal cycle based on HALOE measurements (Steil et al., 1998) to take into account NO_y and Cl_y input from N_2O and CFC degradation at higher altitudes.

2.2. Model validation

Since the present paper concentrates on possible future changes of NO_y and O_3, the following comparison focuses on NO_x, NO_y and O_3, to show the abilities of the employed model system.

2.2.1. NO_x and NO_y. An adequate and detailed comparison of simulated NO_y or NO_x concentrations with observations cannot be performed due to the lack of global long-term measurements. Therefore, only qualitative and coarse quantitative model validation can be carried out. A comparison of model data with aircraft NO_x measurements performed within the Swiss NOXAR project (Brunner, 1998; see also Dameris et al., 1998b) showed a fairly good agreement at flight altitudes (200 hPa): ECHAM3/CHEM produced a seasonal cycle with low values of 10 to 40 pptv between 40°N and 60°N in January and high values of 200 to 400 pptv in July, whereas measured values ranged from 10 to 200 pptv and 150 to 500 pptv, respectively (see Fig. 7.6 in Brunner (1998)). The comparison also showed that the model underestimates gradients between NO_x concentrations over sea and land as well as between mid-latitudes and the tropics. The model is able to reproduce summer and autumn enhanced NO_x concentrations over Europe and Siberia.

Several aircraft measurements west of Ireland, performed within the projects "Pollution from Aircraft Emissions in the North Atlantic Flight Corridor" (POLINAT) and "Schadstoffe in der Luftfahrt" (SIL) were compared with ECHAM3/CHEM results for autumn and summer conditions (Köhler et al., 1998). ECHAM3/CHEM reproduced well the height of maximal NO_x values in both seasons. Nevertheless, the high observed variability (10 to 750 pptv) in summer could not be reproduced by the model (275 ± 50 pptv), which results from the coarse horizontal model resolution compared to the very local in-situ measurements.

Global measurements at lower altitudes are even more sparse. Using several measurements Emmons et al. (1997) showed that vertical NO_x profiles are characterized by a C-shape, with high values in the lower troposphere and near the tropopause and much lower concentrations in the middle troposphere (6 to 9 km). This is in qualitative agreement with ECHAM3/CHEM model data (Dameris et al., 1998b). On the basis of the TRACE A project, Jacob et al. (1996), derived vertical profiles for the tropical Pacific in autumn 1992. They found high near-surface (less than 2 km height) NO_x values (400 pptv) over the eastern continent of South America, which dropped off to less than 10 pptv in the mid of the Pacific and increased again over the western part of Africa. The model shows a similar behaviour with 200 to 900 pptv over the eastern part of South America, 5 to 15 pptv in the mid of the ocean, and 100 to 700 pptv over the western part of Africa. Either dataset (observation and model) shows a much more uniform behaviour around 5 km height. However, observations show values of 50 to 100 pptv between South America and Africa, whereas the model has slightly higher values (50 to 90 pptv) over the continents than over the Pacific (15 to 40 pptv).

2.2.2. O_3. Steil et al. (1998) showed that the model is able to reproduce total ozone measurements (Bojkov and Fioletov, 1995) with regard to the ozone hole, mid-latitude springtime ozone maximum, and tropical minimum. However, the model tends to overestimate ozone concentrations in the mid-latitudes of the winter northern lower stratosphere due to a too strong polar vortex, so that stratosphere to troposphere ozone exchange leads to too high values in the winter northern upper troposphere. Steil et al. (1998) also showed that the long-term mean simulated vertical profiles below 300 hPa compare well, i.e., within the 2σ inter-annual variability, with long-term profiles derived from ozone-sounding stations, which has been confirmed by Köhler et al. (1998) on the basis of aircraft measurements (see above).

The one-year ozone climatology derived from aircraft measurements (Brunner, 1998) showed a quite zonal structure in July, with values of 100 to 150 ppbv at 200 hPa between 40°N and 60°N. This is well reproduced by ECHAM3/CHEM (Fig. 7.5, in Brunner (1998)). In January, observations near 200 hPa show strong longitudinal gradients with high values over America (>200 ppbv) and Asia (>150 ppbv) and low values over the North-Atlantic (<100 ppbv). ECHAM3/CHEM reproduces these gradients, but the absolute values are higher by about 100 ppbv. This discrepancy may partly be explained by an interannual variab-

ility of 40 to 120 ppbv (1 σ standard deviation of the monthly mean values at 60°N), which is not regarded in the observational data set. Another reason is certainly the large-scale stratosphere–troposphere exchange, which is overestimated by the model by a factor of 2 (Grewe et al., 1999b), yielding a strong transport of ozone rich air into the upper troposphere, especially between 30°N and 60°N.

This summary of recent inter-comparisons shows that the model is capable to simulate well the intra- and interannual variability of NO_y and O_3 as well as most of the horizontal and vertical patterns for both tropical and mid-latitude regions.

2.3. *Experimental set-up*

Two control experiments (CNTL92 and CNTL15) were carried out as quasi-equilibrium simulations for the time slices 1992 and 2015 (Table 1). They include representative climate forcings due to prescribed SSTs and GHG concentrations (summarized as equivalent CO_2). Observed SSTs were used for the time slice experiments for 1992 (Gates, 1992). For 2015 we used SSTs derived from transient climate experiments with the coupled atmosphere–ocean general circulation model ECHAM4/OPYC3 (Roeckner et al., 1999). The concentration of greenhouse gases follow the IPCC suggestions IS92a (Leggett et al., 1992). A uniform increase in the NO_x surface emissions and a decrease in the stratospheric chlorine loading (Copenhagen Amendment) is regarded. These two experiments have already been described in Dameris et al. (1998a) and Grewe et al. (1999a). Each experiment (Table 1) consists of 10 model years, which were preceded by a sufficiently long (4 years) spin-up period.

In order to separate effects of emission changes and climate change (temperature, precipitation, wash-out rate, etc.) two additional experiments have been designed (EMIS15 and E + H2O + T15). Both experiments employ the same CO_2 concentration and SST as the control experiment for 1992 (CNTL92), i.e., all three experiments have identical meteorology and differ at any timestep only in chemical quantities. The experiments EMIS15 and E + H2O + T15 include the emissions of NO_x and CFCs for the year 2015, but consider differently temperature (i.e., different reaction rates) and water vapour (i.e., different OH-concentrations) in the chemistry module (Table 1). In the experiment E + H2O + T15 temperatures and water vapour mixing ratios used in the chemistry module have additional offsets compared to those employed in the dynamic part, whereas these offsets are not used for EMIS15. These offsets are derived from the difference of the control experiments for 2015 and 1992 calculated on a monthly mean basis at each grid point (Figs. 2c, 2d, 3c, 3d). Therefore, climatological mean values of 2015 temperatures and water vapour mixing ratios are applied in the chemistry module for E + H2O + T15, whereas the values for 1992 are used for the dynamic part, i.e., for transport, wash-out, etc.

Future changes in chemical quantities will be discussed in Section 4 (Figs. 5 to 8) with the use of these experiments. Figs. 5a to 8a depict the background situation for 1992 (CNTL92). The comparison of the two control runs (CNTL15

Table 1. *Experiment description: emissions and temperatures are given as global, annual means*

Name	Year	Surf. NO_x TgN p.a.	lig. NO_x TgN p.a.	CFCs ppbv	N_2O ppbv	CH_4 ppmv	eq.CO_2 ppmv	SST °C	$\overline{T^c}$, $\overline{H_2O^c}$
CNTL92	1992	31.2	4.0	3.2	310	1.69	407	19.41	CNTL92
EMIS15	1992	53.1	5.0	2.7	333	2.04	407	19.41	CNTL92
E + H2O + T15	1992	53.1	5.0	2.7	333	2.04	407	19.41	CNTL15
CNTL15	2015	53.1	5.0	2.7	333	2.04	488	19.73	CNTL15

Surface emissions are taken from Lee et al. (1997) and are scaled linearly to 2015 using IS92a (Leggett et al., 1992). N_2O and CH_4 are estimated according to IS92a and only applied for the chemistry module, the greenhouse gas increase is considered in terms of equivalent CO_2 (eq.CO_2). The future CFC development is based on the Copenhagen Amendment of 1992 (WMO, 1992). CO surface values are not changed. The sea surface temperature is prescribed using a transient climate experiment with the coupled ocean–atmosphere model ECHAM4/OPYC3 (Roeckner et al., 1998). $\overline{T^c}$ and $\overline{H_2O^c}$ describe the mean temperature and water vapour mixing ratios used in the chemical module.

versus CNTL92, Figs. 5d to 8d) shows the change of chemical species due to changes in the emissions and due to changes in climate (process A + B + C). The sensitivity run EMIS15 will give an idea of the importance of the direct effect of changed NO_x and other emissions (process A), when compared to the control experiment CNTL92 (Figs. 5b to 8b). The comparison of the experiments E + H2O + T15 and EMIS15 shows the effect of temperature and water vapour changes directly on the chemistry, i.e., process B (Figs. 5c to 8c). The total effect of climate change will be shown using the experiments CNTL15 and EMIS15, i.e., process B + C (Figs. 5e to 8e), and the effect of changed circulation and clouds (including precipitation) alone can be derived from the model results of CNTL15 versus E + H2O + T15, i.e., process C (Figs. 5f to 8f). All changes in chemical species will be presented here relative to the background situation in 1992 (CNTL92) to allow direct inter-comparisons.

3. Modeled climate change

In this section a detailed description of modeled changes in meteorological parameters (temperature, water vapour, liquid water, precipitation), which are relevant for the chemistry and are caused by a climate change, is given. It is compared to other model studies to give an idea of the reliability of the predicted changes of each parameter. It is a basis for the interpretation of climate change induced changes in the chemistry in Section 4.

3.1. Temperature

Fig. 2 shows the zonal mean temperatures for 1992 (top) and changes to 2015 (bottom) for January (left) and July (right), as calculated with ECHAM3/CHEM (CNTL92 and CNTL15). As already discussed elsewhere (Dameris et al., 1998a; Grewe et al., 1999a) temperature increases of 1 K near the surface and up to 2 K at tropopause levels were found. Against, the stratosphere cools by 1 to 2 K. This change pattern agrees well with coupled atmosphere–ocean model results, which also show strongest temperature increases in the upper tropical troposphere and a stratospheric cooling (Kattenberg et al., 1996; Roeckner et al., 1999). Absolute values are difficult to compare, since the prognosing horizons differ: Using the ECHAM4/OPYC3 model, Roeckner et al. (1999) found a temperature increase in the upper tropical troposphere between 3.5 and 5 K within 50 years (0.07 to 0.1 K/a), which is comparable to 1.5 to 2 K within 23 years (0.07 to 0.09 K/a) derived in the current work. (This agreement is expected, since SSTs used in the present work were derived from Roeckner et al. (1999).) Other model studies showed similar results. In a doubled CO_2 experiment (approximately 70 years from 1990 according to IS92a) Hansen et al. (1997) used the GISS model and derived an increase of 5 to 6 K in the upper tropical troposphere (0.07 to 0.09 K/a). In a transient experiment with an increase in CO_2 of 1% per year, Manabe et al. (1991) derived a temperature increase of 3 K in the same region (0.04 K/a) with the GFDL coupled model. Mitchell et al. (1998) derived an increase of 5 K for 2050 compared to pre-industrial time on the basis of a transient experiment with the coupled HadCM3 model. Due to the experimental design, i.e., steady state versus transient simulations, the steady state simulations show stronger responses.

3.2. Water vapour

Due to the warming of the troposphere an increase in the water vapour mixing ratios are found throughout the whole atmosphere (Fig. 3). The relative increase is strongest in the upper troposphere at 150 hPa to 200 hPa in the tropics (25%, 40 ppmv) and high latitudes at 300 hPa to 400 hPa of the summer hemisphere ($\approx$20%, 10 to 50 ppmv). The increase in water vapour from 1992 to 2015 amounts to 0.8 to 5.4×10^{-6} kg/kg per year in tropical regions between 400 hPa and 200 hPa. Climate models general show a future increase of water vapour (Kattenberg et al., 1996), e.g., 2 to 7×10^{-6} kg/kg per year between 400 and 200 hPa in the tropics (Hansen et al., 1997), and 30 to 70×10^{-6} kg/kg from pre-industrial time to 2050 (Mitchell et al., 1998), comparing well with the findings in the current simulation. Even more simple models derived this result: Toumi et al. (1996) found a 25% increase in the tropical upper troposphere water vapour at 200 hPa when introducing an global increase of 2 K of the near surface air temperature in a 2-D latitude–height

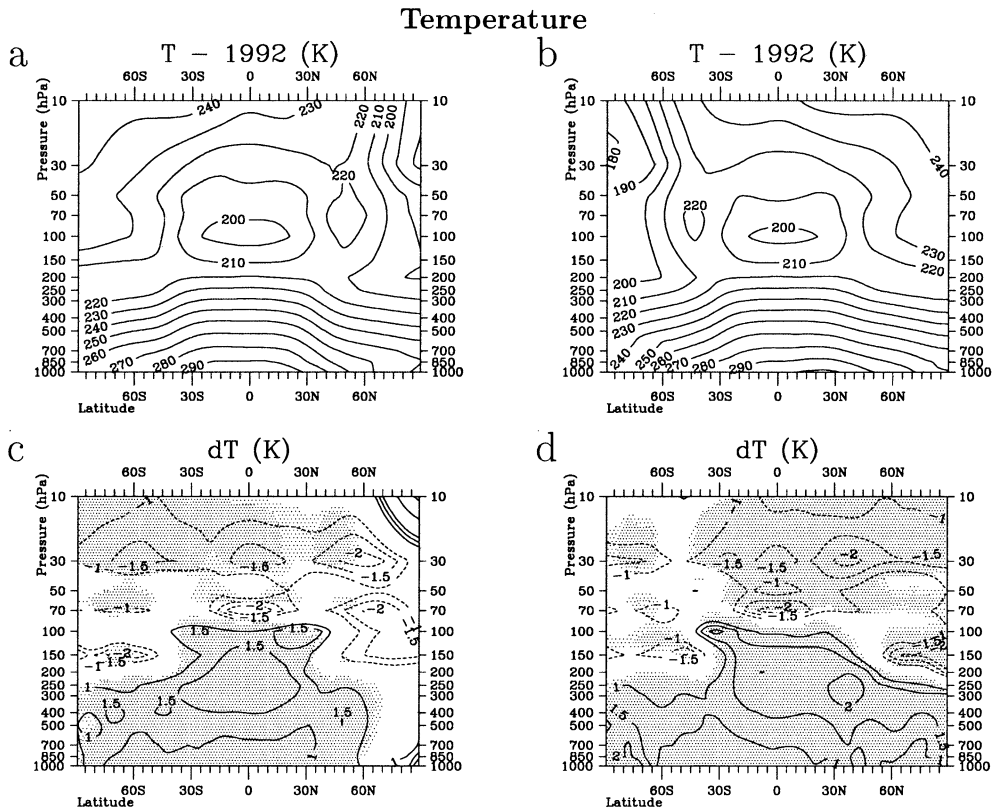

Fig. 2. Zonal mean temperature distribution in 1992 (a, b) and changes to 2015 (c, d) in Kelvin for January (a, c) and July (b, d). Dark (light) shaded areas mark significant changes (univariate *t*-test) on the 99% (95%) level.

troposphere model comparing also well with our findings.

3.3. Liquid water

Fig. 4 shows the model derived liquid water content in 1992 and changes in 2015. A clear increase in the liquid water content is found in the tropical upper (100 hPa to 250 hPa) and extra-tropical middle troposphere (300 hPa to 500 hPa) of 0.1 to 2 ppmv. This increase in the middle and upper troposphere shows the same pattern as the liquid water distribution in the experiment for 1992 (CNTL92). Nevertheless, the relative increase of 10 to 50% is strongest at tropopause levels. Hansen et al. (1997) found a maximum increase of total cloud water content in the tropics of roughly 0.7×10^{-9} kg/kg per year, comparable to the ECHAM3/CHEM simulations, with 0.5×10^{-9} kg/kg per year, nevertheless the pattern differs. Their increase occurs at higher altitudes and is accompanied by a decrease in liquid water content below, down to the surface, which is less pronounced in our simulation. Mitchell et al. (1998) derived a decrease of the annual mean liquid and frozen water content in the middle to upper troposphere tropics.

3.4. Precipitation

Although the general pattern of the future changes of temperature and water vapour agrees well in the various model simulations, the hydrological cycle does not. ECHAM3/CHEM shows a significant increase of the zonal mean total precipitation at northern mid-latitudes throughout the year and an increase (decrease) in the northern (southern) tropics in July. An agreement can be

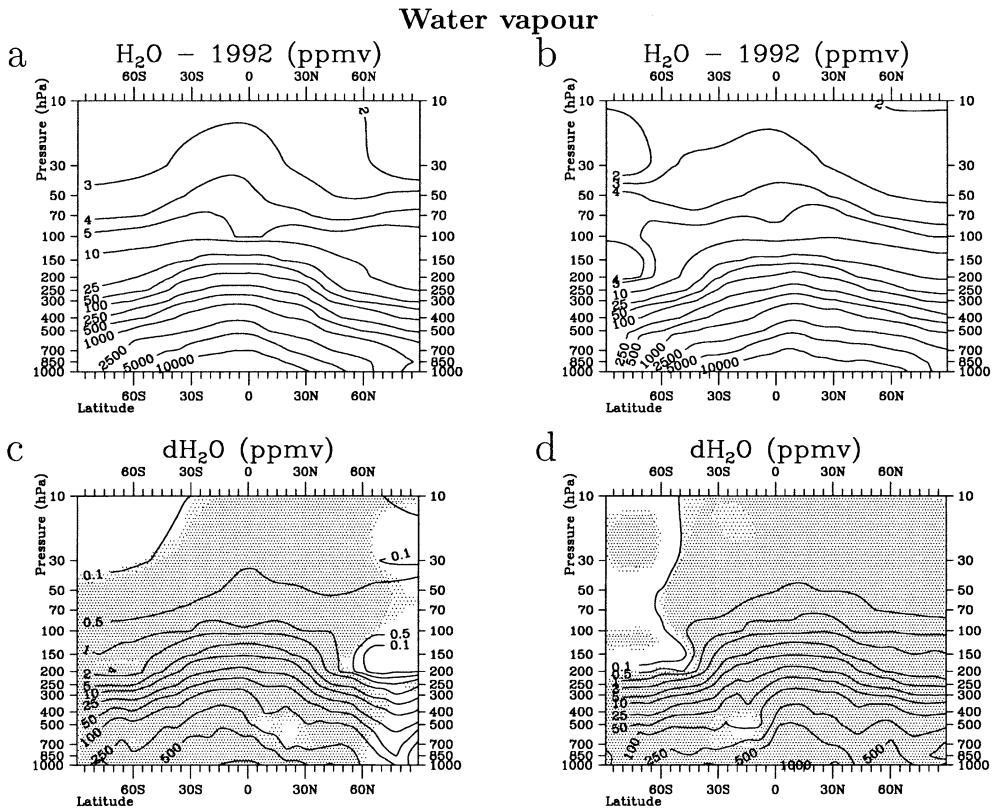

Fig. 3. Zonal mean water vapour volume mixing ratios in 1992 (a, b) and changes to 2015 (c, d) in ppmv for January (a, c) and July (b, d). Dark (light) shaded areas mark significant changes (univariate *t*-test) on the 99% (95%) level.

found with other experiments dealing with longer time intervals (Manabe et al., 1992; Kattenberg et al., 1996; Mitchell et al., 1998; Roeckner et al., 1999; Sabine Brinkop, pers. comm.), concerning the increase of zonal mean precipitation in northern extra tropics. Differences occur in the southern hemisphere and the tropical precipitation patterns. Also the maximum increase of the tropical precipitation differs: 0.05 (January) and 0.01 (July) mm/day per year (Manabe et al., 1992), 0.01 mm/day per year (annual mean) (Roeckner et al., 1999), 0.01 (January) and 0.025 (July) mm/day per year (Sabine Brinkop, pers. comm.), 0.015 (January) 0.025 (July) mm/day per year in the current study, and 1.2 mm/day from pre-industrial times to 2050 (Mitchell et al., 1998).

3.5. *Future climate — Summary*

One can conclude that the temperature and water vapour changes in the troposphere, especially in the upper troposphere agree well with other model results regarding the change pattern and absolute values. Against, the hydrological cycle is simulated differently in various model studies. Nevertheless, there are several agreements, such as the increase in upper troposphere liquid water content and the increase in northern hemisphere winter and tropical precipitation, which has an impact on the modeling of the future atmospheric chemical composition via process C (Fig. 1). Therefore, precipitation, a sink for total nitrogen, is the most uncertain process, which may be changed in a future climate and which influences chemistry.

4. Modeled changes in the atmospheric composition

The atmospheric chemical composition, e.g., the NO_y and O_3 concentrations, depends on various

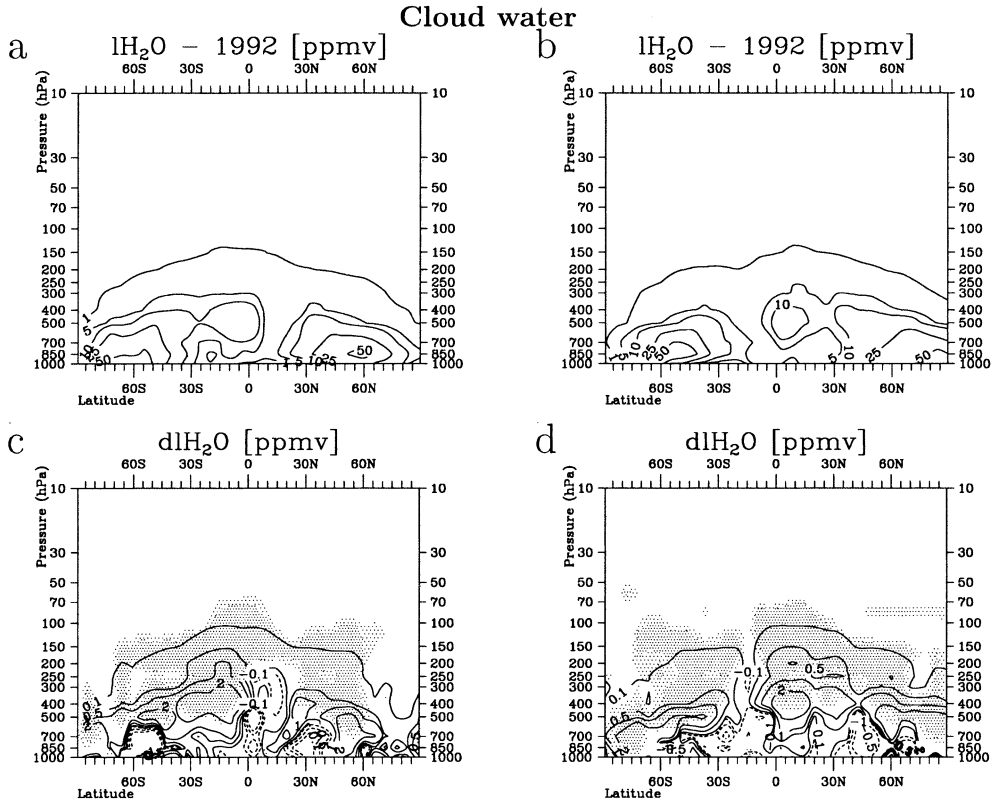

Fig. 4. Zonal mean liquid water given in equivalent water vapour mixing ratios (ppmv) for 1992 (a, b) and changes to 2015 (c, (d) and for January (a, (c) and July (b, d). Dark (light) shaded areas mark significant changes (univariate *t*-test) on the 99% (95%) level

factors. Emissions of NO_x play a major role and directly affect chemistry, whereas the emissions of CO_2 and other greenhouse gases affect dynamics, temperature, clouds and water vapour, which then influence chemistry. In the following these effects will be discussed separately.

4.1. *Direct effect of emissions — process A*

The zonal mean NO_y distributions for January (Fig. 5a) and July (Fig. 6a) of the experiment CNTL92 are dominated by high stratospheric values (>2000 pptv) due to stratospheric N_2O degradation and relative high values (>400 pptv) in the northern lower troposphere caused by NO_x emissions. Low tropospheric NO_y mixing ratios (<100 pptv) are found in the southern hemisphere. A clear seasonal cycle can be seen in the troposphere reflecting the stronger vertical mass exchange in the summer extra-tropics due to convection. A validation of the model data has been provided in Subsection 2.2.

The assumed increase of NO_x and N_2O emissions from 1992 to 2015 (Table 1) leads to an enhancement of total nitrogen (NO_y) in the whole atmosphere (Figs. 5b, 6b), taking into account only direct emission effects, i.e., no changes in the atmospheric dynamics are allowed (experiment EMIS15 versus CNTL92). Largest relative changes of approximately 60% occur near the tropopause in January and July. Similar results are found for NO_x and HNO_3 (not shown). The NO_y partitioning in the troposphere slightly changes: the share of HNO_3 increases by up to 5% points whereas NO_x decreases.

The increase of nitrogen oxide leads to an

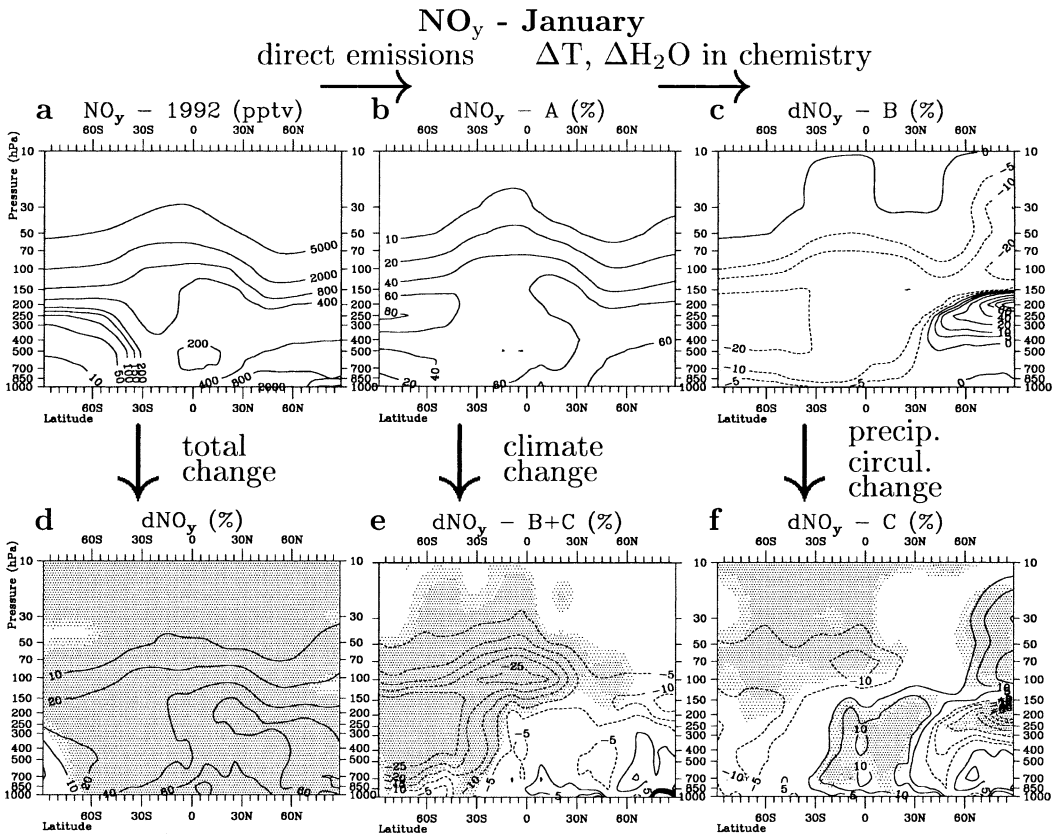

Fig. 5. Zonal mean NO_y mixing ratio (a) for January 1992 in ppbv and changes due to process A (b), B (c), C (f), B + C (e), and changes to 2015 (d) relative to the mixing ratios for January 1992 in %. The Figs. are based on the experiments (a) CNTL92, (b) (EMIS15–CNTL92)/CNTL92, (c) (E + H2O + T15–EMIS15)/CNTL92, (d) (CNTL15–CNTL92)/CNTL92, (e) (CNTL15–EMIS15)/CNTL92, and (f) (CNTL15–E + H2O + T15)/CNTL92. The sum of the numbers given for the processes A (b), B (c), and C (f) gives the total change viewed in (d).) Due to the identical meteorology the changes in b and c are highly significant everywhere, in d, e, and f dark (light) shaded areas mark significant changes (univariate *t*-test) on the 99% (95%) level.

enhancement in the ozone production via photochemical ozone smog reactions (Fishman and Crutzen, 1978; for dependences of the ozone production from atmospheric conditions see Lin et al., 1988; Grooet al., 1998). The main reaction is $NO + HO_2 \rightarrow NO_2 + OH$, followed by photolysis of NO_2 and reaction with molecular oxygen to produce ozone. This results in an increase of the ozone mixing ratio between 20% and 25% throughout the troposphere with only a slight seasonal variation (Figs. 7b, 8b). It also leads to an increase of tropospheric OH of up to 20% in the upper tropical troposphere for January and July. The OH increase leads to a decrease in the methane concentration and to a decrease of the annual mean tropospheric methane lifetime of 7.8%.

As already discussed in the introduction, the 5 CTMs used for the IPCC (1999) show a tropospheric increase in O_3 of 1.8 to 2.1 TgO_3 per emitted TgN for the period from 1992 to 2015. Comparing the experiments EMIS15 and CNTL15 with the experiment CNTL92, here we derive values of 2.2 and 1.8 TgO_3/TgN, respectively. Driving ECHAM3/CHEM in a CTM-like mode, i.e., without a changing climate (EMIS15),

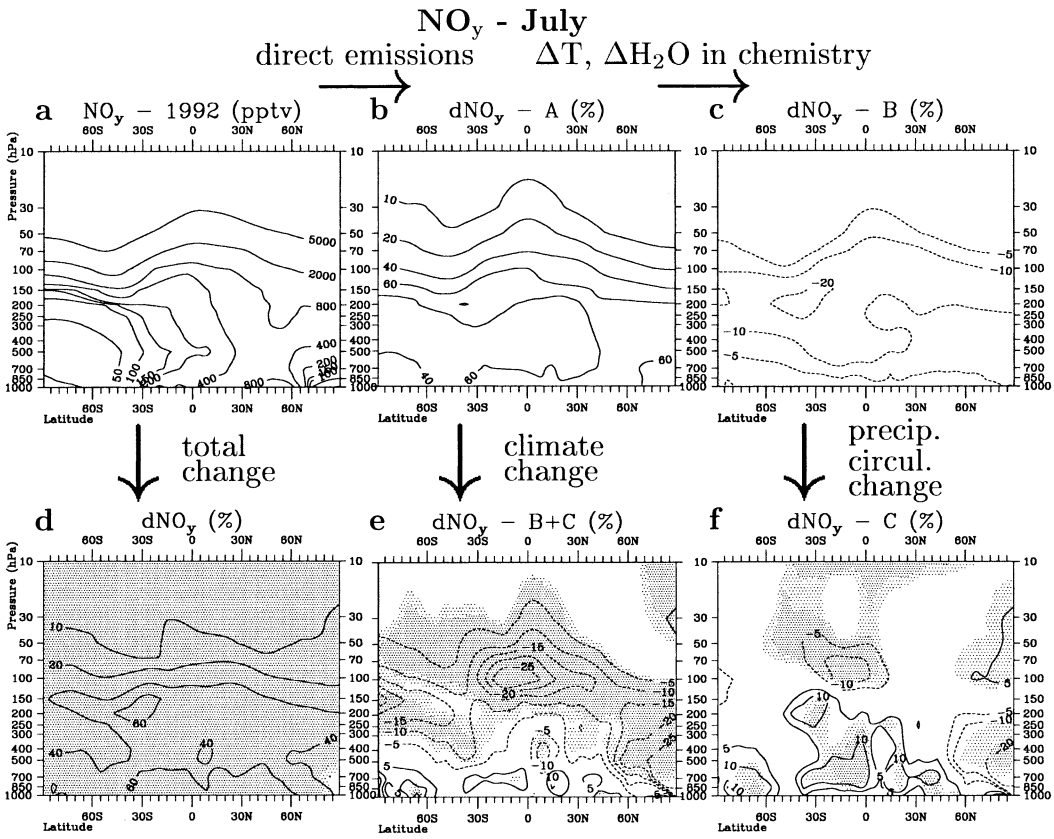

Fig. 6. As Fig. 5, but for July.

it shows a stronger ozone increase than the 5 CTMs, including climate change (CNTL15), it shows the smallest ozone changes.

Johnson et al. (1999) compared a 12 months experiment, which represents the climate of 2075 (doubled CO_2), but with the NO_x emissions of 1990 (2MET, therein), with a control experiment for 2075 including both climate and emissions for 2075 (BOTH, therein). They found an ozone increase of 5 to 15 ppbv in the Northern Hemisphere from 700 to 300 hPa in January and 15 to 25 ppbv in July. These results can be compared with the experiments EMIS15 and CNTL92, which show an increase of 10 to 15 ppbv for January and July, and therefore a much less pronounced seasonal cycle. Relative to the increase in surface NO_x emissions (44.5 TgN/a in HADAM2b/STOCHEM for 1990 to 2075 and 21.5 TgN/a in ECHAM3/CHEM for 1992 to 2015) the HADAM2b/STOCHEM results are lower by a factor of at least 2. Two reasons can be given for this: (1) At higher NO_x concentrations the ozone production per extra NO_x molecule generally decreases (Lin et al., 1988), leading to lower ozone production rates per NO_x emission. (2) In the warmer and more humid climate in 2075 compared to 2015 a lower tropospheric NO_x residence time can be expected, due to higher wash-out rates. Additionally, spin-up effects cannot be excluded, as HADAM2b/STOCHEM takes into account 3 months, whereas ECHAM3/CHEM's spin-up time is at least 2 years to derive quasi-steady state. Since non-methane hydrocarbons (NMHC) are not included in ECHAM3/CHEM this may also partly account for the differences. NMHCs react with OH and lead to HO_2 formation and thus increase the ozone formation in polluted ares (Houweling,

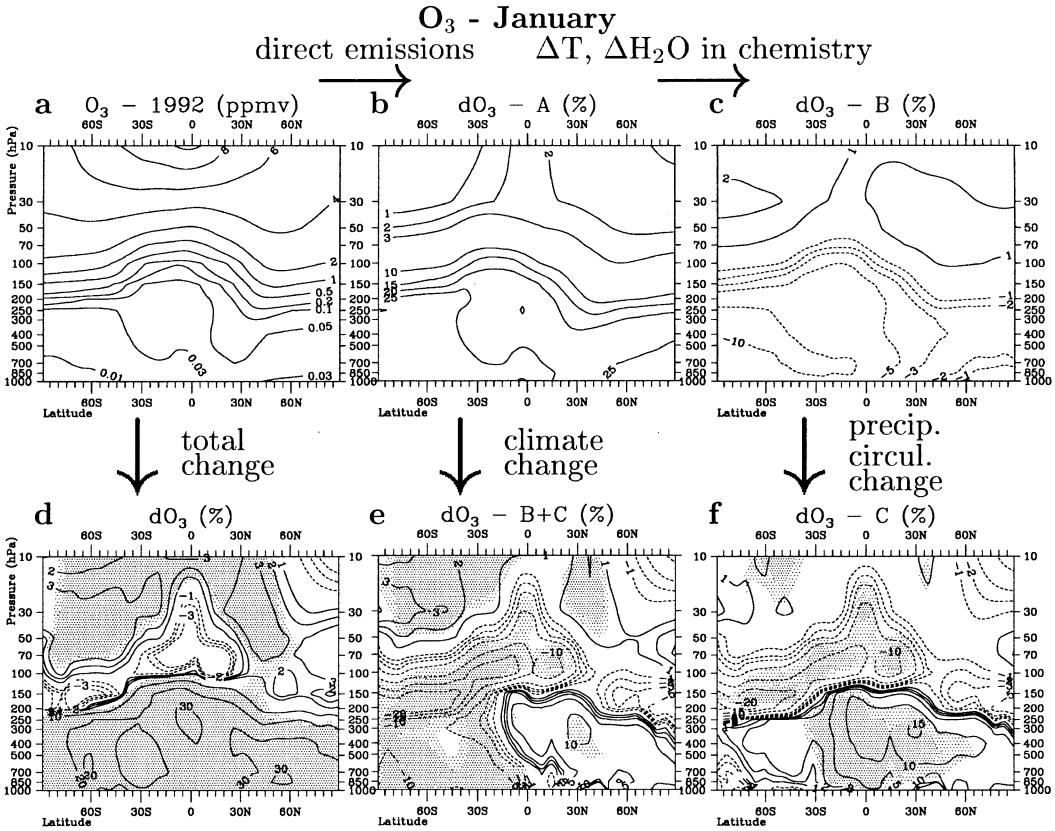

Fig. 7. As Fig. 5, but for O_3.

1999). Including NMHC-chemistry would therefore lead to a higher ozone production in the base case (CNTL92). Increasing NO_x emissions (like in the simulation EMIS15) would probably lead to enhanced PAN formation and could yield a lower increase of the ozone production compared to the base case. On the other hand the thermal decomposition and photolysis of PAN often occurs far away from the source regions, i.e., in regions with low NO_x concentrations. In those regions the ozone production rates can be increased in the high NO_x emissions scenario. The total effect is hard to estimate.

At higher altitudes ECHAM3/CHEM shows much higher ozone values (up to 100 ppbv at 100 hPa) than HADAM2b/STOCHEM, since ECHAM3/CHEM also includes changes in stratospheric ozone, which HADAM2b/STOCHEM does not account for. Total ozone increase in the HADAM2b/STOCHEM model is about 1.7 TgO_3/TgN if a climate change is neglected and 0.9 TgO_3/TgN if climate change is regarded. Again, ECHAM3/CHEM shows higher values and the effect of climate change is less pronounced, but a detailed comparison cannot be performed, since time horizon and experimental set-up differs significantly. However, this model comparison suggests that ECHAM3/CHEM calculates future ozone changes comparable to other chemical transport models and shows qualitatively similar results like the climate-chemistry model HADAM2b/STOCHEM.

4.2. *Indirect effect of temperature and water vapour changes — process B*

Emissions of chemical relevant species affect directly the composition of the atmosphere as shown above, but this impact can be strengthened or weakened by changes in climate. The effect of

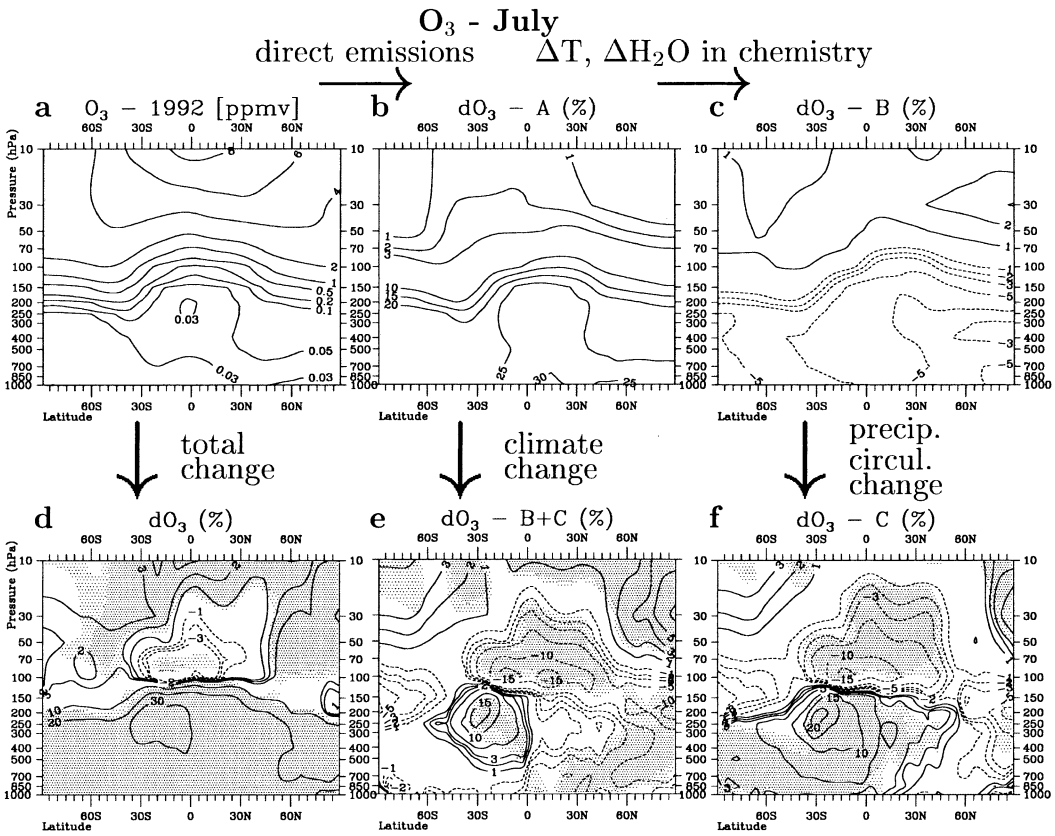

Fig. 8. As Fig. 7, but for July.

temperature changes and water vapour changes due to an increase of greenhouse gas concentrations on the chemical composition is investigated using experiment E + H2O + T15.

Figs. 5c, 6c show the change of the NO_y concentration (experiment E + H2O + T15 versus EMIS15; process B) relative to the background situation (CNTL92). A decrease of the NO_y concentration is found for January and July throughout the whole atmosphere, peaking at −10% to −20% between 100 hPa and 200 hPa, except at 200 hPa in mid- and high northern latitudes in January, where a strong increase is found. We cannot exclude that this increase results from an experimental artifact: Although the meteorology (circulation, cloud water, precipitation) is identical in the experiments E + H2O + T15 and EMIS15 the formation of polar stratospheric clouds and NAT-particles and their sedimentation, which is part of the chemical module, is not. Due to the temperature and water vapour offset applied in the chemistry module in experiment E + H2O + T15, these fields do not correspond to other dynamic parameters, e.g., the location of the polar night jet and the polar vortex. This experimental (not model) artifact, which cannot be avoided, may only occur in highly variable regions with regard to temperature and winds, and where PSC formation occurs, i.e., in northern stratosphere winter. The vertical redistribution of NO_y due to this artificial sedimentation of NAT-particles could be an explanation for the increase at 200 hPa indicated in Fig. 5c. When applying 2015 temperatures and water vapour mixing ratios in a consistent way, this signal is reversed (Fig. 5f), which supports this thesis.

However, this experimental artifact does not occur in other regions, i.e., the decrease in NO_y in the troposphere and lower stratosphere peaking at −20% reflects a change in the NO_y sinks, since

NO_y sources have not been changed. As the meteorology in both experiments (E + H2O + T15 and EMIS15) is identical, i.e., also the precipitation, the NO_y sinks can only be modified by a change in the NO_y partitioning in favour of an increase of the HNO_3 concentration which then leads to higher wash-out even with the same meteorology. Large-scale precipitation is the most important wash-out process in mid- and high northern latitudes. In the northern hemisphere the OH concentration increases by up to 5% in the whole troposphere in summer and at mid-latitudes in winter (not shown). This leads to an increase of the HNO_3 production by the reaction $NO_2 + OH \rightarrow HNO_3$.

In July, the increase of the HNO_3 production leads to a change of the NO_y partitioning. The share of HNO_3 is increasing by 1% leading to an increased wash-out, i.e., leading to a quite effective sink of HNO_3 and NO_y. It results in a change of the HNO_3 and NO_y mixing ratio by -10% to -20%.

The climate change induced temperature and water vapour increases lead to an increase of OH, an increase of the share of HNO_3, and a stronger sink for HNO_3. It results in a decrease of NO_y and also NO_x. This effects tropospheric net ozone production, which decreases and yields a change of the tropospheric ozone abundance by -3% to -5% in the northern hemisphere (Figs. 7c, 8c). The net ozone production is mainly constrained by the counteracting reactions $O_3 + HO_2 \rightarrow 2O_2 + OH$ (ozone loss) and $NO + HO_2 \rightarrow NO_2 + OH$ (leading to ozone production via photolysis and reaction with O_2). Therefore the importance of the changed ozone production and destruction due to climate change induced temperature and water vapour changes can be estimated by looking at the changes due to these reactions. In fact, ozone destruction increases and ozone production decreases at mid-latitudes at 500 hPa, where net ozone production peaks with more than 15×10^4 cm^{-3} s^{-1}. However ozone production decreases $30\times$ stronger than ozone destruction increases, so that the changes in NO, namely NO_x, lead to the changes in ozone.

This means that tropospheric warming and increases in the water vapour mixing ratios partly compensates the increase in tropospheric NO_y and O_3 concentrations due to the direct effect of emissions: The increase in tropospheric NO_y by 40% to 60% is reduced by 5% to 20% and the increase in tropospheric O_3 by 20% to 30% is reduced by 3% to 10%.

Toumi et al. (1996) applied a more simple 2-D general circulation model and increased the surface temperature by 2 K, yielding an increase in parameterized water vapour mixing ratios by 10% to 40%. This results in an annual mean ozone decrease of 2.5% in the southern extra-tropical troposphere, 3% to 5% in the tropical troposphere, and an increase in the northern extra-tropics by up to 3%. Although the temperature increase is twice as strong as in the present simulation, the tropical water vapour and ozone relative changes are similar. Against, ozone changes in the northern hemisphere disagree even in sign. Nevertheless, Toumi et al. (1996) and the present work show that an ozone decrease due to water vapour and temperature increase can be expected in most areas.

4.3. Indirect effect of changes in precipitation and other dynamic parameters — process C

Figs. 5f and 6f show the effects of the change in dynamic/climatic parameters, except temperature and water vapour changes, i.e., process C (Fig. 1), on the NO_y distribution for January and July, respectively. Only some areas are significantly perturbed: In the tropical middle and upper troposphere an increase of 10% is simulated for both seasons. At northern high latitudes, the decrease near the tropopause in January (-50%) is probably disturbed by the experimental artifact discussed above. In July a decrease of -20% in the middle troposphere is found. The tropical lower stratosphere shows a decrease in NO_y mixing ratios of 10% in both seasons.

The tropospheric NO_y increase in the tropical region can be attributed to a change in the hydrological cycle, i.e., precipitation, and wash-out rates: The precipitation increases between 20°S and the equator (the equator and 20°N) and decreases between the equator and 20°N (20°S and the equator) in January (July) in 2015 compared to 1992. Between 500 hPa and 100 hPa the liquid water content and the water vapour increase by up to 50% and 25%, respectively, in those regions, where precipitation increases (Figs. 3, 4). Whereas in those tropical regions, where precipitation decreases, no significant change in the liquid water

content and only a small increase in water vapour is found. The decrease in precipitation and unchanged liquid water content is accompanied by an increase in HNO_3 and NO_y mixing ratios, suggesting a decrease in wash-out rates. The increase in precipitation and enhanced liquid water content yields no significant changes in HNO_3 and NO_y mixing ratios or even an increase, suggesting a saturation of the wash-out rates, e.g., due to fewer but stronger convective events.

At high latitudes an increase of the precipitation is found for July, which is accompanied with an increase in liquid water content (Fig. 4). This leads to an increased wash-out of HNO_3, reducing the HNO_3 share on the NO_y partitioning, as well as the HNO_3 and NO_y mixing ratios. To summarize, tropospheric NO_y increases in tropical regions, where precipitation decreases. Tropospheric NO_y decreases at high latitudes, where precipitation increases.

In the tropical lower and mid troposphere OH increases by up to 5% in January and July, mainly because more NO is available to convert HO_2 into OH by the reaction $NO + HO_2 \rightarrow NO_2 + OH$. In this region it is approximately half of the increase due to process A, where only emissions were increased. It shows that process C may have a significant impact on the tropical oxidation capacity. This has a direct impact on the methane lifetime (decrease by 5.2%), since the tropics and lower latitudes determine the methane destruction.

The tropical tropospheric increase of NO_y is accompanied by an increase of O_3 of 10% to 20% (Figs. 7f, 8f), but since the ozone production rates decrease nearly globally in the troposphere in both seasons (not shown), transport processes must be responsible for the tropospheric ozone increase, which even over-compensate the decrease in the chemical net ozone production. Due to the ozone to NO concentration ratio of less than 2×10^{-4} (Crutzen, 1995) the tropical lower and middle troposphere is dominated by a chemical net ozone destruction in the experiment CNTL92 in January and July. An increase in NO_y and decrease of CO leads to a stronger chemical net ozone destruction.

In the lower tropical stratosphere a decrease of ozone of 5% to 15% is simulated for both seasons, which is not well understood. Nevertheless several processes can be excluded: (1) Chemical ozone destruction, since the net ozone production rate even increases due to processes B and B + C by 5 to 25×10^3 cm^{-3} s^{-1}. (2) Self-healing effect due to a recovery of the tropical ozone layer, because this should be also visible regarding process A, which cannot be seen in Figs. 7b, 8b. (3) Precipitation and wash-out effects can be excluded in that area. Possible explanations are a strengthening of the air mass transport from the stratosphere to troposphere and an increased meridional circulation. The stratosphere to troposphere large-scale exchange peaks around 35°S and 35°N (Grewe and Dameris, 1996; Grewe et al., 1999b). Figs. 7f, 8f support this, since an increase of ozone is found in the upper troposphere in those regions. Against, an increase of the meridional transport of ozone to the winter pole is not supported, since an increase of ozone at high latitudes is not found. However, this can be superimposed by an increase in ozone destruction at mid-latitudes.

4.4. *Summary: Combined direct and indirect effects — processes A, B, and C*

The comparison of ECHAM3/CHEM results for 1992 and 2015 conditions indicate that the processes A, B, and C described above lead to an increase in tropospheric NO_y of more than 40% in January and July. Surface emissions (process A), mainly NO_x, contribute most to this increase. Nevertheless, increase in temperature and water vapour mixing ratios (process B) lead clearly to a decrease in the tropospheric NO_y mixing ratios especially at tropopause levels by more than 10%. Changes in precipitation and liquid water content (process C) caused an increase of 10% in the NO_y mixing ratios in tropical troposphere. The regional pattern of the changes due to processes B and C are very different, so that the total changes due to climate change (process B + C), although of less importance than the direct emission effect (process A), is a relevant and a non-negligible process for the chemical atmospheric composition.

Johnson et al. (1999) found a decrease of tropospheric ozone of 5% in January and July in a $2 \times CO_2$ experiment (2MET, therein) compared to a $1 \times CO_2$ experiment (CON, therein), both with the same NO_x emissions (Fig. 3a, 4a, therein). This agrees with our results only in the summer hemispheric troposphere (Fig. 7e, 8e). However, their model (HADAM2b/STOCHEM) excludes stratospheric chemistry and the model results are

based on 1 year simulations. As shown in Fig. 7e and 8e statistical significance could not be derived for the whole troposphere even for 10 year simulations. Furthermore, as discussed in Subsection 4.1, NMHC-chemistry, which is not included in ECHAM3/CHEM, may also account for the differences.

The tropospheric increase (decrease) of NO_y due to process A (B) yields an increase (decrease) of the absolute values of the ozone production rates with no change in its pattern and an increase (decrease) of the ozone mixing ratios. Dynamic effects (process C), i.e., transport processes, lead to an increase in tropospheric ozone and a decrease in tropical lower stratospheric ozone.

The OH concentration increased in the whole troposphere due to increasing emissions from 1992 to 2015 (EMIS15, process A) and the methane lifetime decreased (−7.8%). The ECHAM3/CHEM simulations show that climate change (process B + C) may even increase the OH concentration in the lower and mid tropical troposphere by up to 5% leading to a decreasing methane lifetime (−4.8%).

5. Conclusions

The climate-chemistry model ECHAM3/CHEM has been applied to estimate future (2015 in comparison to 1992) changes of the chemical atmospheric composition, especially the NO_y and ozone concentrations. It has been shown that the model is able to reproduce the main characteristics of NO_y and ozone concentrations of the present (1992) atmosphere. A simulation of the future atmosphere, considering expected changes in greenhouse gases, sea surface temperatures and emissions of NO_x, CFCs and others has been performed. A global increase in the NO_y and ozone mixing ratios has been found (Figs. 5d, 6d, 7d, 8d), with two exceptions for ozone: (1) The model simulations showed no significant changes or even a significant decrease in ozone in the lower stratosphere between 100 hPa and 30 hPa in the tropics and between 200 hPa and 100 hPa in the extra-tropics. (2) In both polar winter hemispheres, no significant changes were found for stratospheric ozone due to a delay of the ozone recovery caused by a stratospheric cooling (Dameris et al., 1998a).

For a better understanding of these changes, the modeling of the future atmosphere has been performed stepwise. In a first step the emissions of NO_x and other species have been adapted to 2015, which showed a clear increase in tropospheric NO_y and ozone, as expected. In a second step the air chemistry has been changed towards the expected situation in 2015 with respect to air temperature and water vapour content. This lead almost in the whole atmosphere to a decrease of NO_y and a tropospheric ozone decrease and stratospheric ozone increase. In a third step also other dynamic parameter were adapted to the situation simulated for 2015. We showed that those tropical areas, which are accompanied by a decrease of precipitation in 2015 relative to 1992, are also accompanied by an increase in tropical tropospheric ozone of 10%. We argued that the decrease of precipitation leads to a decreased HNO_3 washout, which gives a consistent picture. However, photolysis rates are also effected by this process and may also have an impact on the results. It also turned out that a change of transport processes in the lower stratosphere in 2015 with respect to 1992 is much more important for NO_y and ozone than the increase in surface emissions. It yields a decrease of NO_y and ozone by up to 25%, which out-weights the increase due to the direct emission effects at these altitudes.

This clearly shows that the direct emission effect plays a major rôle in the development of the future chemical composition of the atmosphere. Nevertheless, there is a relevant reduction of the direct emission effect due to expected future temperature and water vapour changes and changes in the circulation of the lower stratosphere.

The intercomparison of different model results for future atmospheric changes (Section 3) suggests that changes in the chemistry due to temperature and water vapour (process B) are more reliable than those due to precipitation and circulation changes (process C). However, process C has the potential to significantly change the atmospheric abundance of NO_y and ozone.

Certainly, a limitation of the model is the absence of NMHC-chemistry and the fixed surface values of CO and CH_4. However this model study requires a coupled climate-chemistry model, which is able to simulate various situations on a ten year basis with reasonable turnaround times on the computer. Therefore no NMHC-chemistry is

included and surface values are prescribed for long-lived species to avoid long spin-up times.

NMHC-chemistry may lead to smaller ozone increases of future ozone production rates, as discussed in Subsection 4.1. Including NMHC-chemistry will certainly change quantitatively the results. However, it is unlikely that the inclusion of NMHC-chemistry will change the main results, e.g., that climate change processes, others than the change in atmospheric water vapour and temperature, have the potential to effect significantly tropical and sub-tropical NO_y and ozone values. Fixed surface values of CO and CH_4 lead to smaller changes in CH_4 due to changes in OH when compared to model runs using surface emissions. Consequently, too much peroxiradicals (HO_2 and CH_3O_2) are produced and the ozone production rates are overestimated over continental areas, compensating somehow the missing NMHC-chemistry.

The future scenarios simulated in the present investigation are based on various input parameters. The increase of well-mixed greenhouse gases follows IPCC recommendations. Changes in the SSTs are prescribed on the basis of a coupled ocean–atmosphere simulation. We showed that the simulated future changes in the main meteorological parameters are consistent with other climate simulations. Uncertainties regarding future NO_x emission scenarios are hard to estimate. The scenarios used for the present investigation are based on the assumption of spatial uniform changes. Fuglestvedt et al. (1999) showed that the effect of NO_x emissions on ozone and on methane lifetime largely depend on its localisation. The quantitative assessment of future changes of the chemical composition of the atmosphere requires a model system with both, a more detailed description of chemical processes than that of ECHAM3/CHEM and the inclusion of climate change processes like in ECHAM3/CHEM.

6. Acknowledgments

This study was funded by the EU within the projects "AEROCHEM" and "AEROCHEM2". We acknowledge very much the support of Erich Roeckner and Monika Esch for providing the SSTs and Christine Coghlan from the Hadley Centre, U.K., who made results from the coupled experiments available for inter-comparison.

REFERENCES

Bojkov, R. D. and Fioletov, V. E. 1995. Estimating the global ozone characteristics during the last 30 years. *J. Geophys. Res.* **100**, 16,537–16,551.

Brasseur, G., Hitchman, M. H., Walters, S., Dymek, M., Falise, E. and Pirre, M. 1990. An interactive chemical dynamical radiative two-dimensional model of the middle atmosphere. *J. Geophys. Res.* **95**, 5639–5655.

Brasseur, G. P., Kiehl, J. T., Müller, J.-F., Schneider, T., Granier, C., Tie, X. X. and Hauglustaine, D. 1998. Past and future changes in global tropospheric ozone: Impact on radiative forcing. *Geophys. Res. Lett.* **25**, 3807–3810.

Brunner, D. 1998. One-year climatology of nitrogen oxides and ozone in the tropopause region. *Results from B-747 aircraft measurements*. PhD thesis, 181 pp., Swiss Federal Institute of Technology (ETH), Zürich, Switzerland.

Crutzen, P. J. 1995. An overview of atmospheric chemistry. In: *Topics in atmospheric and interstellar chemistry*. European Research Course on Atmospheres, ERCA Vol. 1, eds. C. Boutron, 63–88, Les Ulis, France.

Crutzen, P. J. and Zimmermann, P. H. 1991. The changing photochemistry of the troposphere. *Tellus* **43A/B**, 136–151.

Dameris, M., Grewe, V., Hein, R. and Schnadt, C. 1998a. Assessment of the future development of the ozone layer. *Geophys. Res. Lett.* **25**, 3579–3582.

Dameris, M., Grewe, V., Köhler, I., Sausen, R., Brühl, C., Grooß, J.-U. and Steil, B. 1998b. Impact of aircraft NO_x-emissions on tropospheric and stratospheric ozone. Part II: 3-D model results. *Atmos. Environ.* **32**, 3185–3200.

Dentener, F. J. and Crutzen, P. J. 1993. Reaction of N_2O_5 on tropospheric aerosols: Impact on global distributions of NO_x, O_3, and OH. *J. Geophys. Res.* **98**, 7149–7163.

Emmons, L. K., Carroll, M. A., Hauglustaine, D. A., Brasseur, G. P., Atherton, C., Penner, J., Sillman, S., Levy II., H., Rohrer, F., Wauben, W. M. F., van Velthoven, P. F. J., Wang, Y., Jacob, D., Bakwin, P., Dickerson, R., Doddridge, B., Gerbig, C., Honrath, R., Hübler, G., Jaffe, D., Kondo, Y., Munger, J. W., Torres, A. and Volz-Thomas, A. 1997. Climatologies of NO_x and NO_y: Comparison of data and models. *Atmos. Environ.* **31**, 1851–1904.

Fishman, J. and Crutzen, P. J. 1978. The origin of ozone in the troposphere. *Nature* **274**, 853–858.

Fishman J., Ramanathan, V., Crutzen, P. J. and Liu, S. C. 1979. Tropospheric ozone and climate. *Nature* **282**, 818–820.

Fuglestvedt, J. S., Berntsen, T. K., Isaksen, I. S. A., Mao, H., Liang, X.-Z. and Wang, W.-C. 1999. Climatic forcing of nitrogen oxides through changes in tropospheric ozone and methane; global 3D model studies. *Atmos. Environ.* **33**, 961–977.

Gates, W. L. 1992. AMIP: The atmosphere model intercomparison project. *Bull. Amer. Meteor. Soc.* **73**, 1962–1970.

Grewe, V. and Dameris, M. 1996. Calculating the global mass exchange between stratosphere and troposphere. *Ann. Geophys.* **14**, 431–442.

Grewe, V. and Dameris, M. 1997. Heterogeneous PSC ozone loss during an ozone mini-hole. *Geophys. Res. Lett.* **24**, 2503–2506.

Grewe, V., Dameris, M., Sausen, R. and Steil, B. 1998. Impact of stratospheric dynamics and chemistry on northern midlatitude ozone loss. *J. Geophys. Res.* **103**, 25,417–25,433.

Grewe, V., Dameris, M., Hein, R., Köhler, I. and Sausen, R. 1999a. Impact of future subsonic NO_x emissions on the atmospheric composition. *Geophys. Res. Lett.* **26**, 47–50.

Grewe, V., Rogers, H., Pyle, J. and Sausen, R. 1999b. Stratosphere–Troposphere-Exchange. In: *AEROCHEM Final Report*, ed. I. Isaksen, ENV4-CT95-0144EUR, Luxemburg, 44–49.

Grooß, J.-U., Brühl, C. and Peter, T. 1998. Impact of aircraft NO_x-emissions on tropospheric and stratospheric ozone. Part I: Chemistry and 2-D model results. *Atmos. Environ.* **32**, 3173–3184.

Hanson, D. and Mauersberger, K. 1988. Laboratory studies of nitric acid trihydrate: Implications for the south polar stratosphere. *Geophys. Res. Lett.* **15**, 855–858.

Hansen, J., et al. 1997. Forcings and chaos in interannual to decadal climate change. *J. Geophys. Res.* **102**, 25,679–25,720.

Hough, A. M. and Derwent, R. G. 1990. Changes in global concentration of tropospheric ozone due to human activities. *Nature* **344**, 645–648.

Houweling, S. 1999. *Global modeling of atmospheric methane sources and sinks*. PhD thesis, University of Utrecht, Netherlands, 171 pp.

IPCC (Intergovernmental Panel on Climate Change). 1996. *Climate change 1995*, eds. J. T. Houghton, L. G. Meira Filho, B. A. Callander, N. Harris, A. Kattenberg and K. Maskell, Cambridge University Press, New York.

IPCC (Intergovernmental Panel on Climate Change). 1999. Special report on aviation and the global atmosphere, ed. J. T. Houghton, Cambridge University Press, New York.

Jacob, D. J., Heikes, B. G., Fan. S.-M., Logan, J. A., Mauzerall, D. L., Bradshaw, J. D., Singh, H. B., Gregory, G. L., Talbot, R. W., Blake, D. R. and Sachse, G. W. 1996. Origin of ozone and NO_x in the tropical troposphere: A photochemical analysis of aircraft observations over the South Atlantic basin. *J. Geophys. Res.* **101**, 24,235–24,250.

Johnson, C. E., Collins, W. J., Stevenson, D. S. and Derwent, R. G. 1999. The relative roles of climate and emission changes on future tropospheric oxidant concentrations. *J. Geophys. Res.* **104**, 18,631–18,645.

Kattenberg, A., Giorgi, F., Grassl, H., Mehl, G. A., Mitchell, J. F. B., Stouffer, R. J., Tokioka, T., Weaver, A. J. and Wigley, T. M. L. 1996. Climate models — Projections of future climate. In: *Intergovernmental Panel on climate change* (IPCC), *Climate change 1995*, eds. J. T. Houghton, L. G. Meira Filho, B. A. Callander, N. Harris, A. Kattenberg and K. Maskell, Cambridge University Press, New York, 285–358.

Köhler, I., Sausen, R., Grewe, V. and Ziereis, H. 1998. Intercomparison of global model simulations and aircraft measurements in the NAFC. In: *Pollution from aircraft emissions in the North Atlantic flight corridor (POLINAT 2)*, ed. U. Schumann, EUR 18877 EN, Luxemburg, 217–232.

Lee, D. S., Köhler, I., Grobler, E., Rohrer, F., Sausen, R., Gallardo-Klenner, L., Olivier, J. J. G., Dentener, F. J. and Bouwman, A. F. 1997. Estimations of global NO_x emissions and their uncertainties. *Atmos. Environ.* **31**, 1735–1749.

Leggett, J., Pepper, W. J. and Swart, R. J. 1992. Emissions scenarios for the IPCC: an update. In: *Climate change 1992. The supplementary report to the IPCC scientific assessment*, eds. J. T. Houghton et al., Cambridge University Press, Cambridge, U.K., 69–95.

Lin, X., Trainer, M. and Liu, S. C. 1988. On the nonlinearity of the tropospheric ozone production. *J. Geophys. Res.* **93**, 15,879–15,888.

Manabe, S., Stouffer, R. J., Spelman, M. J. and Byan, K. 1991. Transient responses of a coupled ocean–atmosphere model to gradual changes of atmospheric CO_2. Part I: Annual mean responses. *J. Climate* **4**, 785–818.

Manabe, S., Spelman, M. J. and Stouffer, R. J. 1992. Transient responses of a coupled ocean–atmosphere model to gradual changes of atmospheric CO_2. Part II: Seasonal response. *J. Climate* **5**, 105–126.

Mitchell, J. F. B., Johns, T. C. and Senior, C. A. 1998. *Transient response to increasing greenhouse gases using models with and without flux adjustment*. Hadley Centre for Climate Prediction and Research, Technical Note 2, 26 pp, Bracknell, United Kingdom.

Ramanathan, V., Callis, L., Cess, R., Hansen, J., Isaksen, I., Kuhn, W., Lacis, A., Luther, F., Mahlman, J., Reck, R. and Schlesinger, M. 1987. Climate-chemistry interactions and the effects of changing atmospheric trace gases. *Rev. Geophys.* **25**, 1441–1482.

Rasch, P. J. and Williamson, D. L. 1990. Computational aspects of moisture transport in global models of the atmosphere. *Q. J. Roy. Meteorol. Soc.* **116**, 1071–1090.

Roeckner, E., Arpe, K., Bengtsson, L., Brinkop, S., Dümenil, L., Esch, M., Kirk, E., Lunkeit, F., Ponater, M., Rockel, B., Sausen, R., Schlese, U., Schubert, S. and Windelband, M. 1992. *Simulation of the present-day climate with the ECHAM model:*

Impact of model physics and resolution. Rep. 93, Max-Planck-Inst. für Meteorol., Hamburg, Germany.

Roeckner, E., Bengtsson, L., Feichter, J., Lelieveld, J. and Rodhe, H. 1999. Transient climate change simulations with a coupled atmosphere–ocean GCM including the tropospheric sulfur cycle. *J. Climate* **12**, 3004–3042.

Roelofs, G.-J. and Lelieveld, J. 1995. Distribution and budget of O_3 in the troposphere calculated with a chemistry general circulation model. *J. Geophys. Res.* **100**, 20,983–20,998.

Roelofs, G.-J., Lelieveld, J. and Feichter, J. 1999. *Model simulations of the changing distribution of ozone and its radiative forcing of climate: past, present, and future.* Rep. 283, Max-Planck-Inst. für Meteorol., Hamburg, Germany.

Shindell, D. T., Rind, D. and Lonergan, P. 1998a. Climate change and the middle atmosphere. Part IV: Ozone response to doubled CO_2. *J. Climate* **11**, 895–918.

Shindell, D. T., Rind, D. and Lonergan, P. 1998b. Increased polar stratospheric ozone losses and delayed eventual recovery owing to increasing greenhouse-gas concentrations. *Nature* **392**, 589–592.

Steil, B. 1999. *Modellierung der Chemie der globalen Strato- und Troposphäre mit einem drei-dimensionalen Zirkulationsmodell.* PhD thesis, 205 pp., Max-Planck-Inst. für Meteorol., Examensarbeit Nr. 62, Fachbereich Geowissenschaften, Univ. Hamburg, Hamburg, Germany.

Steil, B., Dameris, M., Brühl, C., Crutzen, P. J., Grewe, V., Ponater, M. and Sausen, R. 1998. Development of a chemistry module for GCMs: First results of a multi-annual integration. *Ann. Geophys.* **16**, 205–228.

Stevenson, D. S., Johnson, C. E., Collins, W. J., Derwent, R. G., Shine, K. P. and Edwards, J. M. 1998. Evolution of tropospheric ozone radiative forcing. *Geophys. Res. Lett.* **25**, 3819–3822.

Tiedtke, M. 1989. A comprehensive mass flux scheme for cumulus parameterization in large-scale models. *Mon. Wea. Rev.* **117**, 1779–1800.

Toumi, R., Haigh, J. D. and Law, K. S. 1996. A tropospheric ozone-lightning climate feedback. *Geophys. Res. Lett.* **23**, 1037–1040.

Wang, C. and Prinn, R. G. 1997. Interactions among emissions, atmospheric chemistry, and climate change: Implications for future trends. *MIT Joint program on the science and policy of global change*, **25**.

Wang, C. and Prinn, R. G. 1999. Impact of emissions, chemistry, and climate on atmospheric carbon monoxide: 100-year predictions from a global chemistry-climate model. *Chemosphere Global Change Science* **1**, 77–81.

WMO (World Meteorological Organization). 1992. *Scientific assessment of ozone depletion: 1991.* WMO Rep. 25, Geneva, Switzerland.

Wuebbles, D. J. 1996. Three-dimensional chemistry in the greenhouse. *Climatic Change* **34**, 397–404.